Photoinduced energy transfer between water-soluble CdTe quantum dots and aluminium tetrasulfonated phthalocyanine

Mopelola Idowu,[a] Ji -Yao Chen[ab] and Tebello Nyokong*[a]

Received (in Montpellier, France) 23rd May 2007, Accepted 14th September 2007
First published as an Advance Article on the web 28th September 2007
DOI: 10.1039/b707808k

Thiol stabilized CdTe quantum dots (QDs) synthesized in aqueous phase were used as energy donors to aluminium tetrasulfonated phthalocyanine (AlTSPc) through fluorescence resonance energy transfer (FRET). Energy transfer occurred from the QDs to AlTSPc upon photoexcitation of the QDs. An enhancement in efficiency of energy transfer with the nature of the carboxylic thiol stabilizers on the QDs was observed. The results showed that for enhanced FRET to occur, the donor–acceptor distance has to be lower than the critical distance. The quenching constant K as well as the binding constant k_b values were calculated suggesting strong interaction of the QDs with the AlTSPc. Study of the photophysics of AlTSPc in the presence of the QDs revealed a high triplet state yield, hence the possibility of using QDs in combination with phthalocyanines as photosensitizers in photodynamic therapy. The triplet state lifetimes of AlTSPc in the presence of the QDs were calculated and the lifetime in the presence of CdTe capped with 3-mercaptopropionic acid (MPA) was found to be the longest. MPA capped QD in a mixture with AlTSPc resulted in long triplet lifetime and high triplet yield of the latter, and high energy transfer efficiency, hence was found to be most suitable as a potential candidate for photodynamic therapy of cancer studies.

Introduction

Quantum dots (QDs) are semiconductor nanocrystals which are very attractive because of their small size, photostability and emission tunability compared to conventional dyes. They have been extensively studied in the past and are continuously being exploited since they have potential in biological labeling, optoelectronics and applications in photodynamic therapy.[1–7] Due to their unique physical properties, they can be tuned to have spectral overlap with a particular acceptor thereby donating energy to such acceptors.

Metal phthalocyanines (MPcs) have been a focus of attention because they exhibit exclusive properties. They have shown potential for applications in different fields such as xerographic photoreceptors,[8] infrared sensors,[9] optical recording,[10] organic photoelectronic devices,[11] nonlinear optics,[12] and in photodynamic therapy (PDT) of cancer.[13–19] Their exceptional stability, intense absorption in the red region of the visible spectrum, selective localization in tumors, effective singlet oxygen generation, coupled with their non-toxicity (in the absence of light) and low skin photosensitizing potency, have been considered advantageous for their use in photodynamic therapy.[14–19]

Photodynamic therapy (PDT) is an emerging modality for the treatment of different types of cancer. It combines the selectivity of fibre optic directed light with the cell destruction properties of singlet oxygen. MPc complexes are promising as photosensitizers for PDT, due to their intense absorption in the red region of visible light. It is believed that during PDT, the photosensitizer is excited to its triplet state, and then transfers its energy to ground state oxygen, O_2 ($^3\Sigma_g$), generating excited state oxygen, $^1O_2$ ($^1\Delta_g$), which is the chief cytotoxic species, through the so-called Type II mechanism.[20] The selectivity of this treatment is unparalleled since only tissues that are simultaneously exposed to the photosensitizer and light, in the presence of oxygen are the ones affected by the cytotoxicity during PDT.[21–23] Alternatively, there can be an indirect activation of the photosensitizer by photoluminescent quantum dots through energy transfer to the photosensitizer. Studies on the ability of QDs to transfer energy to organic dyes have recently attracted attention.[24,25]

There are many methods of synthesizing QDs,[26,27] but most are in organic solvents. Growth of quantum dots in high boiling solvents such as dimethylformamide (DMF) proceeds faster, however such QDs are incompatible to aqueous bioassay conditions. Thus there is a need for water-soluble QDs.[3] QDs have been coupled to non-water-soluble photosensitisers,[7] to give hydrophobic QD–Pc conjugates which were reported to have promising characteristics for PDT. However, for real PDT applications, water solubility is necessary, so, it is desirable to couple them (water-soluble QDs) to water-soluble MPcs. Herein, hydrophilic QD–AlTSPc conjugates with different linkers (Fig. 1(a)) were studied spectroscopically. The transfer of energy emitted by QDs to aluminium tetrasulfonated phthalocyanine (AlTSPc) (Fig. 1(b)) will be discussed. The use of different thiols was undertaken since the nature of the capping thiol affects the particle growth and the emission efficiency of the QDs.[28] The characteristic of AlTSPc at the

[a] *Department of Chemistry, Rhodes University, Grahamstown, 6140, South Africa. E-mail: t.nyokong@ru.ac.za; Fax: +27 46 6225109; Tel: +27 46 6038260*
[b] *Department of Physics, Fudan University, Shanghai, 200433, China*

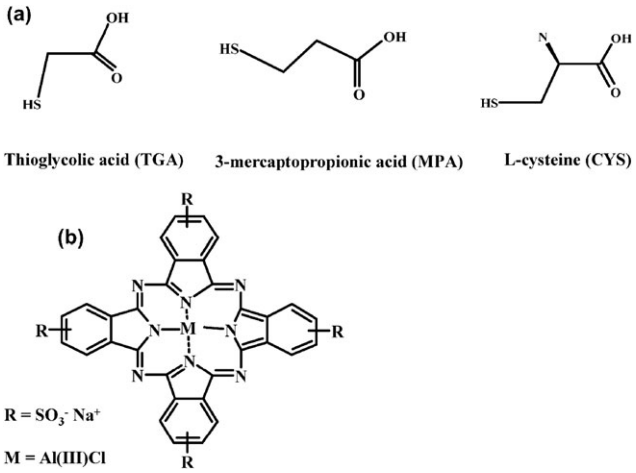

Fig. 1 Molecular structures of (a) thiol-ligands used in capping CdTe quantum dots and (b) aluminium tetrasulfonated phthalocyanine.

triplet state in the presence of the QDs was also studied and the rate of binding of the QDs to AlTSPc was monitored.

Results and discussion

Synthesis, absorption and fluorescence spectra of QDs

The QDs were synthesized in aqueous media to give hydrophilic conjugates capped with thiols, as opposed to the more common synthesis in organic media.[7] The thiols chosen were thioglycolic acid (TGA), 3-mercaptopropionic acid (MPA) and L-cysteine (CYS). The QDs particles grow during the course of the heating of the mixture of thiols, $CdCl_2 \cdot H_2O$ and H_2Te, as a result of the quantum confinement effect. The emission spectra of the CdTe quantum dots began to appear after 5–10 min of refluxing. The spectra continued to shift until there was overlap between the emission spectra of QDs and the absorption spectra of AlTSPc. Two types of QDs are presented in this work, depending on their emission spectral region, hence their size and the extent of overlap with the absorption spectra of AlTSPc. The smaller QDs which show emission spectra between 567 and 587 nm (sizes 2.3 to 3.2 nm) are represented with label 1 after the capping thiol as follows: TGA1, MPA1 and CYS1. Those with more red shifted emission spectra (and larger size, 35 to 3.7 nm) ranging from 626 to 632 nm are represented with a label 2 after the capping thiol as follows: TGA2, MPA2 and CYS2.

Typical normalized absorption and photoluminescence spectra of the synthesized quantum dots stabilized with different carboxylic thiol derivatives (Fig. 1(a)) are shown in Fig. 2 and the excitation and emission spectra of AlTSPc shown in Fig. 3. The absorption spectra of the QDs show typical[28] broad peaks in the visible region with tails extending to about 700 nm. The absorption spectra of the synthesized QDs indicate that the CdTe QDs have a wide range of absorption with their absorption peak maxima ranging from 500 to 600 nm as shown in Fig. 2. The absorbance maxima are well resolved in some cases, inferring narrow size distribution of the synthesized QDs.

The emission spectra of the QDs, overlaid with the absorption spectra in Fig. 2, were measured from prepared QDs

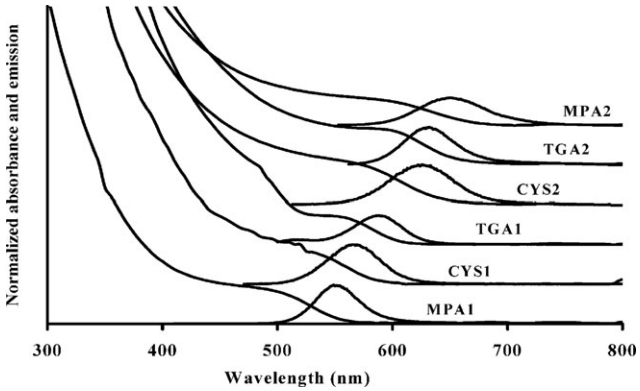

Fig. 2 Absorption and photoluminescence spectra of CdTe quantum dots capped with different thiol carboxylic acids (λ_{exc} = 400 nm); CYS = L-cysteine; MPA = 3-mercaptopropionic acid and TGA = thioglycolic acid capped QDs. pH 7.4 buffer.

solution diluted with pH 7.4 PBS buffer to absorbance of ~0.05 (at the excitation wavelength). The emission spectra are characterized by good symmetry, and are sufficiently narrow with full width at half maximum (FWHM) ranging from 46 to 59 nm as shown in Table 1 for the different QDs. The QDs are photoluminescent in the visible region with the photoluminescence maxima positions ranging from 550 to 649 nm, each having a Stokes' shift around 50 nm. Their band gap energies further proves the quantum confinement effect in QDs. The excitation spectra (Fig. 4), shows sharp peaks on the broad bands compared to the absorption spectra. This is probably due to the reported[28] inhomogeneous broadening which affects the excitation spectra more than the absorption spectra.

Fluorescence quantum yield

Fluorescence quantum yield (Φ_F) values for the CdTe QDs were calculated using eqn (1) and listed in Table 2. The QDs have relatively high quantum yields except for CYS2 whose Φ_F was found to be lowest as shown in Table 2. Except for CYS capped QDs, there is an increase in Φ_F values with increase in the size of QDs (hence with red shifting of the spectra): compare MPA1 with MPA2 and TGA1 with TGA2. The observation of a decrease in Φ_F value for CYS2 compared to CYS1 may be ascribed to the structural differences in these QDs, with CYS2 probably having a less sulfur-enriched

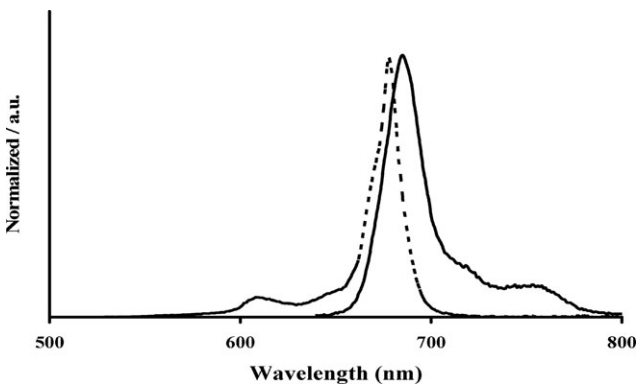

Fig. 3 Spectral features of AlTSPc showing excitation (dashed line) and emission (solid line) spectra. pH 7.4 buffer.

Table 1 Spectral properties of thiol capped CdTe quantum dots (pH 7.4 PBS buffer)

Capping thiol[a]	Size/ nm	$\lambda_{abs.}^{max}$/ nm	λ_{PL}^{max}/ nm	Band gap/eV	FWHM[b]/ nm
CYS1	3.0	530	567	2.17	54
MPA1	2.3	500	550	2.25	46
TGA1	3.2	550	587	2.11	49
CYS2	3.5	578	626	1.98	58
MPA2	3.6	595	649	1.91	59
TGA2	3.7	600	632	1.96	48

[a] CYS = L-Cysteine; MPA = 3-mercaptopropionic acid and TGA = thioglycolic acid. [b] FWHM = Full-width at half maximum (FWHM).

pre-surface layer, hence a low Φ_F value compared to CYS1. Fluorescence quantum yield (excitation at 400 nm) of the QDs ($\Phi_{F(QD)}^{Mix}$) in the mixture of AlTSPc and QDs decreased, Table 2, compared to $\Phi_{F(QD)}$ of QDs alone, indicating strong interaction between the QDs and AlTSPc which will be discussed below. Fluorescence quantum yield (excitation at 630 nm) of the AlTSPc (Φ_{AlTSPc}^{Mix}) in the mixture of AlTSPc and QDs compared to the former alone $\Phi_{F(AlTSPc)}$ = 0.13, remained almost unchanged with the exception of the larger QDs (TGA2 and MPA2), where there was a slight decrease.

Triplet quantum yields (Φ_T) and lifetime (τ_T) studies

Φ_T Values provide a measure of the fraction of absorbing molecules that undergoes intersystem crossing (isc) to the triplet state (Φ_T). The variation of Φ_T values of AlTSPc in the presence of the QDs is shown in Table 2. With the exception of CYS1, the values Φ_T for AlTSPc in the presence of QD are higher than for AlTSPc alone (Φ_T = 0.36). This slight increase in Φ_T in the presence of QDs is attributed to the heavy atom effects of the QDs which contain heavy Cd and Te atoms. The increase in Φ_T of AlTSPc may be advantageous since it means the combination of QDs with phthalocyanines will increase the triplet state character of the phthalocyanine, and so this will give higher photosensitising ability when used

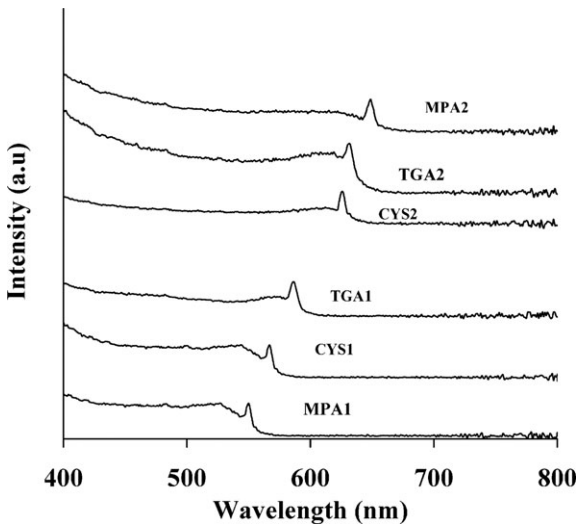

Fig. 4 Excitation spectra of the six CdTe quantum dots capped with different thiol carboxylic acids: CYS = L-cysteine; MPA = 3-mercaptopropionic acid and. TGA = thioglycolic acid capped QDs. pH 7.4 buffer.

Table 2 Fluorescence quantum yields of QDs and photophysical parameters of AlTSPc in the presence of QDs[a] pH 7.4 PBS buffer

Capping thiol[b]	$\Phi_{F(QD)}$[c]	$\Phi_{T(AlTSPc)}^{Mix}$[d]	$\tau_{T(AlTSPc)}^{Mix}$[e]/μs	$\Phi_{F(QD)}^{Mix}$	$\Phi_{F(AlTSPc)}^{Mix}$
CYS1	0.41	0.34	470	0.32	0.12
MPA1	0.19	0.50	740	0.16	0.12
TGA1	0.30	0.45	500	0.26	0.13
CYS2	0.09	0.45	530	0.003	0.10
MPA2	0.59	0.42	570	0.25	0.07
TGA2	0.62	0.42	320	0.40	0.09

[a] legend: $\Phi_{F(QD)}$ = fluorescence quantum yield of QDs alone (excitation = 400 nm); $\Phi_{T(AlTSPc)}^{Mix}$ = triplet quantum yield of AlTSPc in the mixture with QDs; $\tau_{T(AlTSPc)}^{Mix}$ = triplet lifetime of AlTSPc in the mixture with QDs; $\Phi_{F(QD)}^{Mix}$ = fluorescence quantum yield of QDs in the mixture with AlTSPc (excitation 400 nm); $\Phi_{F(AlTSPc)}^{Mix}$ = fluorescence quantum yield of AlTSPc in a mixture with QDs (excitation 630 nm). [b] CYS = L-cysteine; MPA = 3-mercaptopropionic acid and TGA = thioglycolic acid. [c] $\Phi_{F(AlTSPc)}$ = 0.13. [d] $\Phi_{T(AlTSPc)}$ = 0.36. [e] $\tau_{T(AlTSPc)}$ = 470 μs.

together in PDT. In general there is a decrease in Φ_T with increase in the size of the QDs corresponding to the increase in Φ_F (except for the CYS capped QDs), suggesting that the size of the QDs influence the Φ_T for AlTSPc.

Triplet state lifetimes (τ_T) of AlTSPc in the presence of the QDs were relatively high compared to τ_T value of 470 μs for AlTSPc alone, except for CYS1 and TGA2 capped QDs, where, respectively the values were similar or lower. It was observed that the τ_T of the AlTSPc in the presence of CdTe QDs capped with 3-mercaptopropionic (MPA1 and MPA2), had the longest triplet lifetime as seen in Table 2. This may be due to that fact that MPA being a strong coupling agent must have been firmly adsorbed onto the surface of AlTSPc, thereby reducing its exposure to the aqueous medium. The increase in the τ_T of AlTSPc in the presence of QD (for MPA1, MPA2, CYS2, TGA1, Table 2) contradicts what is expected by the heavy atom effect, whereby when Φ_T increases as observed above, the τ_T inevitably decreases. Again with the exception of CYS capped QDs, the τ_T values decreased with increase in the size of the QDs (comparing MPA1 with MPA2 and TGA1 with TGA2). The τ_T value increased with the size of QDs for the CYS capped QDs.

Determination of binding constants and fluorescence quenching

The electronic absorption spectrum of AlTSPc in the presence of QD is shown in Fig. 5. The spectrum is slightly blue-shifted by about 3 nm; this behaviour has been documented before for interaction of QDs with porphyrins.[29] The binding confirms that the quenching between QDs and AlTSPc is static as will be discussed below. It is most likely that the QDs interact with AlTSPc by adsorption.

Fig. 6 shows the fluorescence emission spectra of QD (10^{-6} mol dm^{-3}) in the presence of varying concentrations (0 to 6.18 $\times$ 10^{-6} mol dm^{-3}) of the AlTSPc. The QDs' fluorescence was found to decrease progressively with increasing concentration of AlTSPc. This quenching in fluorescence was used to estimate the binding constants (k_b) and the number of binding sites (n) using eqn (3), with results obtained listed in Table 3. The high values for k_b indicate that there is a relative affinity for AlTSPc by the QDs. The values of k_b for the MPA capped

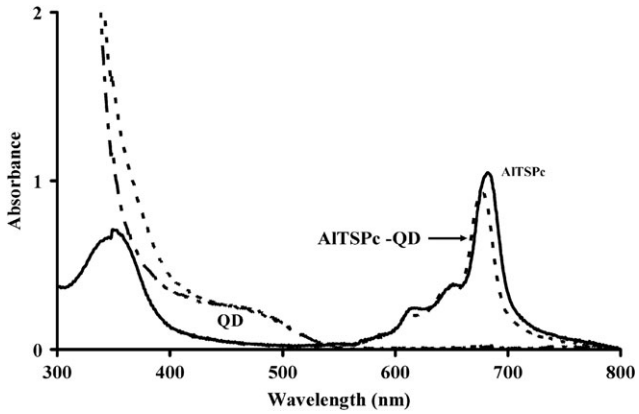

Fig. 5 Absorption spectral changes of AlTSPc (6×10^{-6} mol dm^{-3}) on addition of MPA1 (10^{-6} mol dm^{-3}) in 0.01 M PBS pH 7.4 buffer.

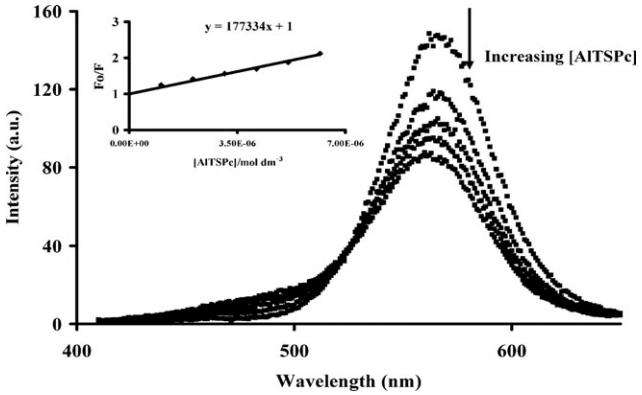

Fig. 6 Fluorescence emission spectral changes of CdTe–CYS (CYS1) with increasing [AlTSPc] in 0.01 mol dm^{-3} PBS pH 7.4. Inset: static quenching plot for AlTSPc quenching of QD ([QD] = 10^{-6} mol dm^{-3} [AlOCPc] = 0 to 6.18×10^{-6} mol dm^{-3}).

QDs conjugates within each set of synthesized QDs were quite high compared to the others suggesting that a strong coupling may be occurring between MPA and AlTSPc. The value of n was found to be $\sim$1. CYS1 and CYS2 gave the lowest k_b values. In all cases CYS capped QDs behave differently from the others, this could be due to the fact that the nature of the thiol strongly influences the particle growth, which would in turn affect their interaction with the photosensitizers, in this case AlTSPc.

The slopes of the plot of F_0/F against [AlTSPc] gave the static quenching constant (K)[30] (eqn (4)) for the fluorescence quenching of the QDs fluorescence with AlTSPc, within investigated range of concentrations and an intercept of 1 (inset Fig. 6). Table 3 lists the K values.

Fluorescence energy transfer study

An efficient overlap between the absorption spectrum of AlTSPc with the emission spectra of the QDs, (Fig. 7), especially for the larger QDs (with more red shifted absorption) was observed. A decrease in the fluorescence emission (on exciting at 400 nm) of the QDs on interacting with AlTSPc and an observation of the AlTSPc fluorescence with a peak at 692 nm was also observed in Fig. 8, suggesting that the quenching of CdTe QDs by AlTSPc involves energy transfer, as was also observed in Fig. 6. The quenching is expected to be *via* energy transfer since AlTSPc absorbs at a longer wavelength than the CdTe QDs. No significant fluorescence for AlTSPc was observed on excitation at this wavelength (400 nm) in the absence of QDs. As stated above, fluorescence quantum yield of the QDs in the mixture of AlTSPc and QDs ($\Phi^{Mix}_{F(QD)}$) decreased for all the conjugates compared to $\Phi_{F(QD)}$ of QDs alone, indicating strong interaction between the QDs and AlTSPc.

The shaded portion in Fig. 7 shows the spectral overlap of fluorescence spectrum of each QD with the absorption spectrum of AlTSPc. The overlap integral (J) was estimated by integration of the spectra in Fig. 7 from 400 to 800 nm and the J values are reported in Table 3. Relatively high J values of the order of 10^{-13} were obtained, (with CYS2 having the highest value) compared to typical values of the order 10^{-14}.[31] This could be as a result of the immense spectral overlap of the absorption spectra of the AlTSPc and the fluorescence emission spectra of the QDs. The Förster distance, R_0 (Å) which is the critical distance between the donor and the acceptor molecules for which efficiency of energy transfer is 50%[32] is also shown in Table 3. The center-to-center separation distance between donor and acceptor (r, Å), were calculated using eqn (7) and values are shown in Table 3 with CYS2 having the lowest values compared to the others. The distances are <80 Å,[33] which indicates that the energy transfer from the synthesized QDs to the AlTSPc occur with high probability. In the smaller first set of QDs, MPA1, CYS1 and TGA1, little FRET is expected since the average distance between the donor and the acceptor r exceeds the critical distance R_0, this is also the case in TGA2. Using eqn (7), the FRET efficiency was calculated with values stated in Table 3. FRET efficiency is a function of the inter-fluorophore distance and spectral properties of donor and acceptor (fluorescence quantum yields, molar absorptivities and relative orientation of transition moments). It is apparent from the results in Table 3, that the CdTe QDs capped with L-cysteine (CYS1 and CYS2) had the

Table 3 Binding, quenching and energy transfer parameters for AlTSPc-QD interactions in pH 7.4 PBS buffer

Capping thiol[a]	$10^{-5}k_b$/mol^{-1} dm^3	n	$10^{-5}K$/mol^{-1} dm^3	$10^{13}J$/cm^6	R_0/Å	r/Å	*Eff*
CYS1	0.61	0.89	1.77	1.37	46.57	57.52	0.22
MPA1	1.62	1.07	0.62	1.08	39.39	52.06	0.16
TGA1	0.89	0.97	1.21	1.73	46.09	62.38	0.14
CYS2	0.34	0.94	0.68	13.9	44.69	25.04	0.97
MPA2	11.6	1.15	1.69	8.2	72.81	68.99	0.58
TGA2	6.43	1.09	1.80	9.75	69.21	76.73	0.35

[a] CYS = L-Cysteine; MPA = 3-mercaptopropionic acid and TGA = thioglycolic acid.

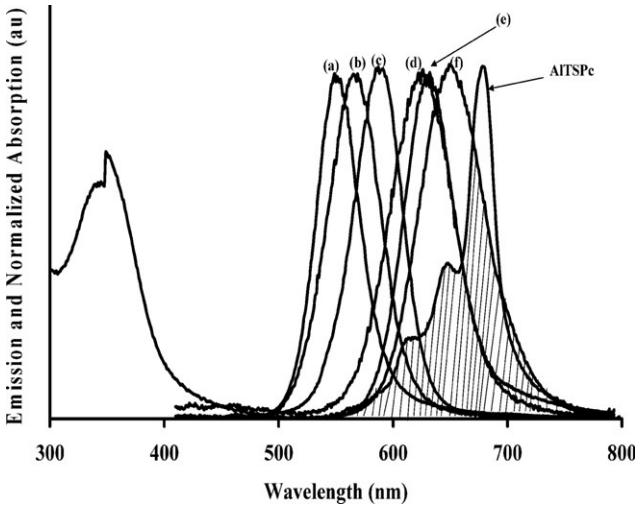

Fig. 7 Normalized absorption spectra of AlTSPc and photoemission spectra of the six CdTe thiol capped QD solutions showing overlap of the emission spectra of the QDs (λ_{exc} = 400 nm) with the absorption spectra of AlTSPc: (a) MPA1, (b) CYS1, (c) TGA1, (d) CYS2, (e) TGA2 and (f) MPA2.

highest efficiency in each set of synthesized QDs (0.22 for CYS1 and 0.97 for CYS2) followed by the 3-mercaptopropionic capped CdTe QDs with the thioglycolic acid capped CdTe QDs having the lowest efficiency for each set. This brings up the possibility that the nature of the thiol stabilizer used in capping the QDs may affect the efficiency of FRET to the AlTSPc. It is also evident that, the QDs with photoluminescence at lower wavelengths, hence smaller QDs (MPA1, CYS1 and TGA1) were less efficient in FRET compared to the larger QDs (red shifted); this is probably due to their low spectral overlap with AlTSPc as compared to the QDs at higher wavelengths of photoluminescence. The high J value coupled with the small r value which is even smaller than R_0 in CYS2 must have all contributed to the high efficiency experienced in CYS2 even though its fluorescence quantum yield is quite low. For the potential use in PDT application, MPA2 capped QD seems to be the suitable water-soluble conjugate with AlTSPc that possesses high energy transfer efficiency (0.58), and also

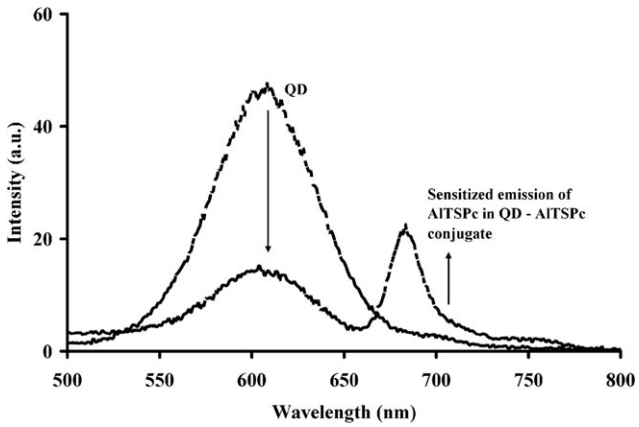

Fig. 8 Indirect activation of AlTSPc through CdTe–Cys (CYS2) QD by FRET showing decrease in CdTe QD emission intensity and a sensitized emission of AlTSPc: λ_{exc} = 400 nm.

the QDs have a relatively high fluorescence yield ($\Phi^{Mix}_{F(QD)}$ = 0.25) in the mixture, that could favor the detection. Although CYS2 linked QD–MPc had the highest efficiency (0.97), this compound resulted in QDs with low $\Phi^{Mix}_{F(QD)}$ (0.003) in the mixture. Thus, the MPA2 linked QD–MPc is a potential candidate for PDT studies in terms of imaging. The next step of *in vitro* PDT work with this compound is being carried out.

Conclusions

Thiol capped CdTe nanoparticles synthesized in aqueous solution have been used as energy donors to water-soluble AlTSPc through a FRET evaluation. We observed an enhancement in efficiency of energy transfer with nature of the carboxylic thiol stabilizers (CYS > MPA > TGA). The donor–acceptor distance was evaluated using Förster theory and it was found that these distances have to be lower than the critical distance for enhanced FRET to occur. Increase in the triplet state quantum yield of AlTSPc in the presence of the QDs was observed and this indicates that photodynamic therapy can be more effective when photosensitizers are attached to QDs. Large binding constant values were obtained suggesting strong interaction of the QDs with AlTSPc; hence this preliminary results illustrate that CdTe QDs prepared in water phase combined with a phthalocyanine derivative probably will become an attractive alternative in photodynamic therapy.

Experimental

Materials

Aluminium tetrasulfophthalocyanine (AlTSPc) was synthesized, purified and characterized according to Weber and Busch method.[34] $CdCl_2 \cdot H_2O$, tellurium powder (200 mesh), thioglycolic acid, 3-mercaptopropionic acid, L-cysteine and Rhodamine 6G were obtained from Sigma-Aldrich. $NaBH_4$, NaOH and H_2SO_4 were obtained from SAARCHEM. Ultra pure water was obtained from a Milli-Q Water System (Millipore Corp, Bedford, MA, USA). Phosphate buffer saline (PBS) solution (0.01 mol dm^{-3}, pH 7.4) was employed.

Synthesis of quantum dots. The preparation of thiol capped QD was performed *via* a modified method adopted from literature.[28,35] Briefly, 2.35 mmol of $CdCl_2 \cdot H_2O$ was dissolved in 125 ml of water and 5.7 mmol of thioglycolic acid (TGA) was added under stirring. The solution was adjusted to pH 12 by addition of NaOH dropwise. Nitrogen gas was bubbled through the solution for about 1 hour. The aqueous solution was reacted with H_2Te gas. H_2Te gas was generated by the reaction of $NaBH_4$ with Te powder in the presence of 0.5 mol dm^{-3} H_2SO_4 under a flow of nitrogen gas. The molar ratio of Cd^{2+} : Te^{2-} : TGA was 1 : 0.5 : 2.4 (Te as powder). A change of colour was observed at this stage. The solution was then refluxed under air at 100 °C for different times to control the size of the CdTe QDs. Different sizes are formed at different reaction times, the solution was continuously sampled to record the emission spectra of the quantum dots until the desired wavelength (hence size) was attained.

The synthesis described above for TGA was also repeated for 3-mercaptopropionic acid (MPA) and L-cysteine (CYS) using the same molar ratio (Cd^{2+} : Te^{2-} : thiol) as for TGA. On cooling, the QDs were precipitated out from solution using excess ethanol; the solutions were then centrifuged to harvest the QDs. The following QDs were selected for study: (i) MPA capped CdTe with emission peaks at 550 nm (MPA1) and at 649 nm (MPA2), (ii) TGA capped CdTe with emission peaks at 587 nm (TGA1) and at 632 nm (TGA2) and (iii) CYS capped CdTe with emission peaks at 567 nm (CYS1) and at 626 (CYS2).

The size of the quantum dots were estimated using the polynomial fitting function derived in the literature.[36] The error in the determination was 5%.

Instrumentation and measurements

Fluorescence excitation and emission spectra were recorded on a Varian Eclipse spectrofluorometer. UV-visible spectra were recorded on a Varian 500 UV-Vis/NIR spectrophotometer. Laser flash photolysis experiments were performed with light pulses produced by a Quanta-Ray Nd:YAG laser providing 400 mJ, 90 ns pulses of laser light at 10 Hz, pumping a Lambda-Physik FL3002 dye (Pyridin 1 dye in methanol). Single pulse energy ranged from 2 to 7 mJ. The analyzing beam source was from a Thermo Oriel xenon arc lamp, and a photomultiplier tube was used as detector. Signals were recorded with a digital real-time oscilloscope (Tektronix TDS 360). The triplet life times were determined by exponential fitting of the kinetic curves using the program OriginPro 7.5.

Photophysical and photochemical studies

Fluorescence quantum yields (Φ_F) were determined by comparative method[37] using eqn (1),

$$\Phi_F = \Phi_{F(R)} \frac{F A_R \eta^2}{F_R A \eta_R^2} \quad (1)$$

where F is the fluorescence intensity, A is the optical density at the excitation wavelength, and η is the refractive index of the solvent used. R refers to the reference fluorophore with known quantum yield. Rhodamine 6G with $\Phi_F = 0.94$[38,39] in ethanol and ZnPc with $\Phi_F = 0.18$[40] in DMSO were employed as standards. Φ_F was determined for both QDs and AlTSPc in water (pH 7.4 buffer). At least three independent experiments were performed for the quantum yield determinations. Both the sample and the reference were excited at the same relevant wavelength.

Triplet quantum yields were determined using a comparative method based on triplet decay, using eqn (2):

$$\Phi_T^{Sample} = \Phi_T^{Std} \frac{\Delta A_T^{Sample} \varepsilon_T^{Std}}{\Delta A_T^{Std} \varepsilon_T^{Sample}} \quad (2)$$

where A_T^{Sample} and A_T^{Std} are the changes in the triplet state absorbance of the sample derivative and the standard, respectively; ε_T^{Sample} and ε_T^{Std} are the triplet state extinction coefficients for the sample and standard, respectively; Φ_T^{Std} is the triplet state quantum yield for the standard. ZnTSPc in aqueous solution, $\Phi_T^{Std} = 0.56$[41] was used as standard. Φ_T, determined for the mixture of QDs and AlTSPc is represented as $\Phi_{T(AlTSPc)}^{Mix}$ and the corresponding triplet lifetime as $\tau_{T(AlTSPc)}^{Mix}$.

Interaction of AlTSPc with QD

The interaction of the AlTSPc with QDs was studied by spectrofluorometry at room temperature. An aqueous solution of QDs (fixed concentration of 10^{-6} mol dm^{-3}) was titrated with varying concentrations (0 to 6.18×10^{-6} mol dm^{-3}) of the AlTSPc solution. The QDs were excited at 400 nm and fluorescence recorded between 400 and 650 nm. The steady decrease in the fluorescence intensity of QDs with increase in AlTSPc concentration was noted and used in the determination of the binding constants and the number of binding sites on QDs, according to eqn (3).[42–44]

$$\log\left[\frac{(F_0 - F)}{F - F_\infty}\right] = \log k_b + n \log[\text{AlTSPc}] \quad (3)$$

where F_0 and F are the fluorescence intensities of QDs in the absence and presence of AlTSPc, respectively; F_∞, the fluorescence intensity of QDs saturated with AlTSPc; k_b, the binding constant; n, the number of binding sites on QDs. Plots of $\log[(F_0 - F)/(F - F_\infty)]$ against log [AlTSPc] provided the values of n (from slope) and k_b (from the intercept). The changes in QD fluorescence intensity were related to AlTSPc concentration by the static quenching equation[45] (eqn (4)):

$$\frac{F_0}{F} = 1 + K[\text{AlTSPc}] \quad (4)$$

where K represents the quenching constant, F_0 and F are the fluorescence intensities of the QDs in the absence and presence of AlTSPc, respectively.

Energy transfer study

The determined fluorescence quantum yield values of AlTSPc and QDs were employed in determining the fluorescence quantum yields of QD in each mixture ($\Phi_{F(QD)}^{Mix}$) using a modified form of eqn (1) as shown by eqn (5).

$$\Phi_{F(QD)}^{Mix} = \Phi_{F(QD)} \frac{F_{QD-AlTSPc}}{F_{QD}} \quad (5)$$

where $\Phi_{F(QD)}$ is the fluorescence quantum yield of the QDs alone, and was used as standard, $F_{QD-AlTSPc}$ is the fluorescence intensity of the mixture when excited at the excitation wavelength of the QDs (400 nm) and F_{QD} is the fluorescence intensity of the QD alone at the same excitation wavelength.

Fluorescence resonance energy transfer (FRET) was also monitored. FRET involves nonradiative energy transfer from a photoexcited donor fluorophore, after absorption of a higher energy photon, to an acceptor fluorophore of a different species which is in close proximity, the donor and acceptor fluorophores may be separated or attached. FRET results from dipole–dipole interactions and is extremely dependent on the center-to-center separation distance between donor and acceptor (r), the degree of spectral overlap of the donor's fluorescence emission spectrum and the acceptor's absorption spectrum and a highly fluorescent donor is important.[31,40] Practically, there is a consequential quenching in the donor photoemission and an increase in the acceptor's fluorescence when FRET has occurred. FRET efficiency (*Eff*) is determined

experimentally from the fluorescence quantum yields of the donor in the absence and presence of the acceptor and it is defined by eqn (6).[31,38,40]

$$Eff = 1 - \frac{\Phi_{F(QD)}^{Mix}}{\Phi_{F(QD)}} \quad (6)$$

There is an inverse 6th order law dependence of *Eff* on *r* due to the dipole–dipole coupling mechanism; hence *Eff* is related to *r* (Å) by eqn (7):[32,38]

$$Eff = \frac{R_0^6}{R_0^6 + r^6} \quad (7)$$

where R_0 (The Förster distance, Å) is the critical distance between the donor and the acceptor molecules for which efficiency of energy transfer is 50% and depends on the quantum yield of the donor, extinction coefficient of the acceptor and all other factors governing FRET as mentioned above.[32,38]

R_0 is expressed by eqn (8):

$$R_0^6 = 8.8 \times 10^{23} \kappa^2 \eta^{-4} \Phi_{F(QD)} J \quad (8)$$

where κ^2 is the dipole orientation factor; η, the refractive index of the medium; Φ_F, the fluorescence quantum yield of the donor in the absence of the acceptor; and J is the Förster overlap integral calculated as (eqn (9)):

$$J = \int f_{QD}(\lambda) \varepsilon_{AlTSPc}(\lambda) \lambda^4 \, d\lambda \quad (9)$$

where f_{QD} is the normalized QD emission spectrum; and ε_{AlTSPc}, the molar extinction coefficient of AlTSPc. In this case, it is assumed that κ^2 is 2/3; such assumption is often made for donor–acceptor pairs in a liquid medium, which are considered to be isotropically oriented during their fluorescence lifetimes. FRET parameters were computed using the program PhotochemCAD.[45]

Acknowledgements

Financial support of this work from Rhodes University and the National Research Foundation (NRF GUN 2053657) of South Africa is gratefully acknowledged. J. Y. C. thanks NSFC (10774027) of China.

References

1 A. P. Alivasatos, *Science*, 1996, **271**, 933.
2 A. P. Alivasatos, *J. Phys. Chem.*, 1996, **100**, 13226.
3 N. Gaponik, I. L. Radtchenko, G. B. Sukhorukov, H. Weller and A. L. Rogach, *Adv. Mater.*, 2002, **14**, 879.
4 M. Han, X. Gao, J. Z. Su and S. Nie, *Nat. Biotechnol.*, 2001, **19**, 631.
5 D. V. Talapin, A. L. Rogach, E. V. Shevchenko, A. Komowski, M. Haase and H. Weller, *J. Am. Chem. Soc.*, 2002, **124**, 5782.
6 H. Mattoussi, J. M. Mauro, E. R. Goldman, G. P. Anderson, V. C. Sundar, F. V. Mikulec and M. G. Bawendi, *J. Am. Chem. Soc.*, 2000, **122**, 12142.
7 A. C. S. Samia, S. Dayal and C. Burda, *Photochem. Photobiol.*, 2006, **82**, 617.
8 M. S. Xu, J. B. Xu, M. Wang and L. Que, *J. Appl. Phys.*, 2002, **91**, 748.
9 L. E. Norena-Franco and F. K. Vasnik, *Analyst*, 1996, **121**, 1115.
10 D. Gu, O. Chen, F. Tang, F. Gan, K. Shen, K. Liu and H. Xu, *Proc. SPIE–Int. Soc. Opt. Eng.*, 1996, **2931**, 67.
11 A. Hagfeldt and M. Gratzel, *Acc. Chem. Res.*, 2000, **33**, 269.
12 M. Calvete, G. Y. Yang and M. Hanack, *Synth. Met.*, 2004, **141**, 231.
13 S. L. Haywood-Small, D. I. Vernon, J. Griffiths, J. Schofield and S. B. Brown, *Biochem. Biophys. Res. Commun.*, 2006, **339**, 569.
14 I. J. Macdonald and T. J. Dougherty, *J. Porphyrins Phthalocyanines*, 2001, **5**, 105.
15 I. Rosenthal, *Photochem. Photobiol.*, 1991, **53**, 859.
16 J. D. Spikes, *Photochem. Photobiol.*, 1986, **43**, 691.
17 J. D. Spikes, *J. Photochem. Photobiol., B*, 1990, **6**, 259.
18 S. G. Brown, C. J. Tralau, P. D. Colendge-Smith, D. Akdemir and T. J. Wieman, Br, *J. Cancer*, 1987, **54**, 43.
19 R. Bonnett, *Chemical Aspects of Photodynamic Therapy*, Gordon and Breach Science Publishers, Amsterdam, 2000.
20 G. Ricciardi, S. Belviso, M. DÁuria and F. Lelj, *J. Porphyrins Phthalocyanines*, 1998, **2**, 517.
21 C. M. Allen, W. M. Sharman and J. E. Van Lier, *J. Porphyrins Phthalocyanines*, 2001, **5**, 161.
22 R. L. Morris, K. Azizuddin, M. Lam, J. Berlin, A. Nieminen, M. E. Kenney, A. C. S. Samia, C. Burda and N. L. Oleinick, *Cancer Res.*, 2003, **63**, 5194.
23 T. J. Dougherty, C. J. Gomer, B. W. Henderson, G. Jori, D. Kessel, M. Korbelik and Q. Peng, *J. Natl. Cancer Inst.*, 1998, **90**, 889.
24 A. R. Clapp, I. L. Medintz, B. R. Fisher, G. P. Anderson and H. Mattoussi, *J. Am. Chem. Soc.*, 2005, **127**, 1242.
25 A. R. Clapp, I. L. Medintz, J. M. Mauro, B. R. Fisher, M. G. Bawendi and H. Mattoussi, *J. Am. Chem. Soc.*, 2004, **126**, 301.
26 Z. G. Ye, M. Q. Tan, G. L. Wang and J. L. Yuan, *Talanta*, 2005, **65**, 206.
27 C. P. Collier, S. Henrichs, J. J. Shiang, R. J. Saykally and J. R. Heath, *Science*, 1997, **277**, 1978.
28 N. Gaponik, D. V. Talapin, A. L. Rogach, K. Hoppe, E. V. Shevchenko, A. Kornowski, A. Eychmuller and H. Weller, *J. Phys. Chem. B*, 2002, **106**, 7177.
29 L. Shi, B. Hernandez and M. Selke, *J. Am. Chem. Soc.*, 2006, **128**, 627.
30 G. Z. Chen, X. Z. Huang and J. G. Xu, *The Analytic Methods of Fluorescence*, Science Press, Beijing, 1990.
31 J. S. Hsiao, B. P. Krueger, R. W. Wagner, T. E. Johnson, J. K. Delaney, D. C. Mauzerall, G. R. Fleming, J. S. Lindsey, D. F. Bocian and R. J. Donohoe, *J. Am. Chem. Soc.*, 1996, **118**, 11181.
32 T. Forster, *Discuss. Faraday Soc.*, 1959, **27**, 7.
33 Y. J. Hu, Y. Liu, R. M. Zhao, J. X. Dong and S. S. Qu, *J. Photochem. Photobiol., A*, 2006, **179**, 324.
34 J. H. Weber and D. H. Busch, *Inorg. Chem.*, 1965, **4**, 469.
35 A. Shavel, N. Gaponik and A. Eychmuller, *J. Phys. Chem. B*, 2006, **110**, 19280.
36 W. W. Yu, L. Qu, W. Guo and X. Peng, *Chem. Mater.*, 2003, **15**, 2854.
37 S. Fery-Forgues and D. Lavabre, *J. Chem. Educ.*, 1999, **76**, 1260.
38 J. R. Lakowicz, *Principles of Fluorescence Spectroscopy*, Kluwer Academic/Plenum Publishers, New York, 2nd edn, 1999.
39 R. F. Kubin and A. N. Fletcher, *J. Lumin.*, 1982, **27**, 455.
40 P. Jacques and A. M. Braun, *Helv. Chim. Acta*, 1981, **64**, 1800.
41 A. Harriman and M. C. Richoux, *J. Chem. Soc., Faraday Trans. 2*, 1980, **76**, 1618.
42 S. Lehrer and G. D. Fashman, *Biochem. Biophys. Res. Commun.*, 1966, **23**, 133.
43 S. M. T. Nunes, F. S. Squilla and A. C. Tedesco, *Braz. J. Med. Biol. Res.*, 2004, **37**, 273.
44 D. M. Chipman, V. Grisaro and N. Sharon, *J. Biol. Chem.*, 1967, **242**, 4388.
45 H. Du, R. A. Fuh, J. Li, L. A. Cockan and J. S. Lindsey, *Photochem. Photobiol.*, 1998, **68**, 141.

